Mon. Not. R. Astron. Soc. **337,** 1340–1348 (2002)

Radiative accelerations on Ne in the atmospheres of late B stars

J. Budaj[1,2]★† and M. M. Dworetsky[1]★

[1] *Department of Physics & Astronomy, University College London, Gower Street, London WCIE 6BT*

[2] *Astronomical Institute, Slovak Academy of Sciences, 059 60 Tatranská Lomnica, The Slovak Republic*

Accepted 2002 August 19. Received 2002 August 15; in original form 2002 April 26

ABSTRACT

Radiative accelerations on Ne are calculated for the atmospheres of main-sequence stars with $11\,000 \leqslant T_{\rm eff} \leqslant 15\,000$ K. This range corresponds to that of the mercury-manganese (HgMn) stars. The calculations take into account neon fine structure as well as shadowing of neon lines using the entire Kurucz line list, bound–bound, bound–free and free–free opacity of H, He and C as well as some non-LTE effects. Non-LTE effects are found to modify the radiative acceleration by a factor of the order of 10^2 in the outer atmosphere and are crucial for d$m < 10^{-3}$ g cm^{-2}. The dependence of the radiative accelerations on the Ne abundance, effective temperature and gravity is studied. Radiative accelerations are found to be well below the gravitational acceleration over the entire range of $T_{\rm eff}$ and it is predicted that in stable atmospheres devoid of disturbing motions, Ne should sink and be observed as under-abundant. This agrees with recent observations of low Ne abundances in HgMn stars.

Key words: stars: abundances – stars: atmospheres – stars: chemically peculiar.

1 INTRODUCTION

Radiatively driven diffusion processes are generally accepted to be responsible for chemical peculiarities observed among upper main-sequence CP stars (Michaud 1970). The upward radiative acceleration and downward gravity acting on different chemical species compete and drive their microscopic diffusion, resulting in the stratification of these elements in the stellar atmospheres or envelopes of these stars. If these atmospheres are sufficiently stable, chemical inhomogeneities can persevere, and are not wiped out by various mixing processes such as convective zones, stellar winds or rotationally induced mixing. In the particular case of HgMn star atmospheres, temperatures are high enough for hydrogen to be largely ionized, thus removing its convection zone. Also, if the He ionization convection zone diminishes owing to He settling in late B stars rotating slower than $\sim$75 km s^{-1} (Michaud 1982; Charbonneau & Michaud 1988), diffusion can operate very effectively in the atmosphere. This is the case for HgMn stars as they are also known as slow rotators. Such diffusion processes are generally time-dependent problems, but the characteristic time-scales in the atmosphere are much shorter than in the envelope ($\leqslant 10^3$ yr) owing to the considerable lower density, smaller collision rates and higher diffusion velocities ($\sim$1 cm s^{-1}). This makes the time-dependent calculations extremely difficult. So far, diffusion can be followed in time only in the envelope, as shown in the case of neon by Seaton (1997, 1999), Landstreet, Dolez & Vauclair (1998) and LeBlanc, Michaud & Richer (2000). These calculations suggest that radiative accelerations on Ne are much lower than those due to gravity below the atmosphere and Ne should sink and be observed as under-abundant unless a weak stellar wind transports upwards the Ne accumulated in deep layers.

Nevertheless, observations are restricted to the atmospheres. This important stellar region bridges the effects in the envelopes with those outside the stars, such as stellar winds, and one clearly also needs to know the radiative accelerations here in order to compare the theory with observations. The case of Ne is worth studying for two reasons: it is an important element having a very high standard abundance (Anders & Grevesse 1989; Grevesse, Noels & Sauval 1996; Dworetsky & Budaj 2000) of about $A(\mathrm{Ne/H}) = 1.23 \times 10^{-4}$, and because one can expect similar effects as in the case of He. Ne I (along with He I) has a very high ionization potential and a first excited level well above the ground state. Ne I is thus the dominant ionization state in the atmospheres of these stars and all Ne I resonance lines are in the Lyman continuum. This part of the spectrum is very sensitive to non-LTE (NLTE) effects and the temperature structure of the atmosphere. It is known that there is a big difference in the temperature behaviour between LTE and NLTE model atmospheres at small optical depths and that temperature can rise outwards in the NLTE models. Ne I is also known to have strong NLTE effects on lines originating from excited levels in the visible part of the spectrum even in late B-type main-sequence stars (Auer & Mihalas 1973; Sigut 1999; Dworetsky & Budaj 2000). Thus, the main complication is clear in performing the task. One cannot rely upon the diffusion approximation when calculating energy flux as this is a non-local quantity in the atmosphere, in contrast to envelope calculations. One needs to solve the radiative transfer as, for example, in Hui-Bon-Hoa, LeBlanc & Hauschildt (2000), Hui-Bon-Hoa,

★E-mail: budaj@ta3.sk (JB); mmd@star.ucl.ac.uk (MMD)
†At UCL during 1999–2000.

Alecian & Artru (1996) or Hui-Bon-Hoa et al. (2002), including NLTE effects if possible.

Unfortunately, observations of Ne in HgMn stars are very scarce and apart from recent LTE Ne abundances in κ Cnc HR7245 and HD29 647 by Adelman & Pintado (2000) and Adelman et al. (2001) the only study of Ne was undertaken recently by Dworetsky & Budaj (2000). Their NLTE analysis of 20 HgMn and five normal stars revealed that Ne is clearly under-abundant in HgMn stars and the deficit reaches its peak values in the middle of the $T_{\rm eff}$ domain of HgMn stars.

In this paper we deal with the radiative accelerations of neon in the atmosphere. This might enable us to model the vertical element stratification in the future, e.g. considering the atmosphere as being in a sequence of stationary states, which are to be tailored to the much more slowly varying envelope as proposed by Budaj et al. (1993). Nevertheless, some conclusions can already be drawn from the radiative accelerations alone. In the following, cgs units and LTE approximations (in a NLTE atmosphere model) are used if not specified otherwise.

2 RADIATIVE ACCELERATION

2.1 Theory

The physics and calculations of radiative accelerations in the envelopes are clearly explained in Seaton (1997), recent improvements are described in Gonzalez et al. (1995) and some theoretical aspects are discussed in Sapar & Aret (1995). Our approach to the problem of calculating accelerations in the atmospheres is described here. Radiative acceleration on the element is caused by the momentum transferred to the element ions from photons absorbed via bound–bound, bound–free and free–free transitions. Bound–bound transitions are usually the most important. An expression for the radiative acceleration on the ion i through its spectral lines can be derived from the radiative transfer equation. For a particular spectral line in the case of complete redistribution we have

$$\mathrm{d}I_\nu = [n_{u,i}A_{ul} - (n_{l,i}B_{lu} - n_{u,i}B_{ul})I_\nu]h\nu\varphi_{lu}(\nu)\,\mathrm{d}s, \tag{1}$$

where the three terms describe spontaneous isotropic emission, absorption and stimulated emission, respectively. Note that stimulated emission is in the direction of the photon absorbed. Here, and in the following, I_ν is the monochromatic intensity, F_ν is the monochromatic energy flux, $h\nu$ is the energy of the transition from the lower level l to the upper level u, $\varphi_{lu}(\nu, \tau)$ is the normalized Voigt profile, τ is the Rosseland optical depth, s is the distance along the beam, $n_{l,i}$ is the NLTE population of the lth state of ith ion, n_i is the total NLTE ith ion population, $b_{l,i}$, $b_{u,i}$ are b-factors defined as a ratio of NLTE to LTE level population ($b_{l,i} \equiv n_{l,i}/n^*_{l,i}$), m is the mass of the ith ion, c is the speed of light, k is the Boltzmann constant and T is the temperature. A_{ul}, B_{ul}, B_{lu} are the Einstein coefficients where B_{lu} is related to the oscillator strength f_{lu} and B_{ul} by

$$B_{lu} = \pi e^2 f_{lu}(m_{\rm e}ch\nu)^{-1}, \quad g_{l,i}B_{lu} = g_{u,i}B_{ul}, \tag{2}$$

where e and $m_{\rm e}$ are the electron charge and mass, respectively, and $g_{l,i}$, $g_{u,i}$ are statistical weights of the lower and upper levels. Introducing the vertical geometrical depth $\mathrm{d}r = \cos\theta\,\mathrm{d}s$, multiplying equation (1) by $\cos\theta\,\mathrm{d}\omega$ and integrating through all solid angles $\mathrm{d}\omega$ we find for the radiation pressure gradient $\mathrm{d}p^{\rm R}_\nu/\mathrm{d}r$:

$$c\frac{\mathrm{d}p^{\rm R}_\nu}{\mathrm{d}r} = -\left(1 - \frac{n_{u,i}}{n_{l,i}}\frac{g_{l,i}}{g_{u,i}}\right) n_{l,i}B_{lu}h\nu F_\nu\varphi_{lu}(\nu). \tag{3}$$

If p_{lu} is the momentum removed from the radiation field through one spectral line in unit volume and a_{lu}, a_i are the corresponding accelerations acquired by the ion i then we obtain

$$a_i(\tau) = \sum_{lu} a_{lu} = \frac{1}{mn_i}\sum_{lu}\frac{\mathrm{d}p_{lu}}{\mathrm{d}t} \quad \text{or} \tag{4}$$

$$a_i(\tau) = -\frac{1}{mn_i}\sum_{lu}\int_0^\infty \frac{\mathrm{d}p^{\rm R}_\nu}{\mathrm{d}r}\,\mathrm{d}\nu. \tag{5}$$

The sum runs through all $l \rightarrow u$ transitions in the ion. Applying the Boltzmann formula to LTE populations, in this general NLTE case, we finally have

$$a_i(\tau) = \sum_{lu}\frac{h\nu}{mc}\left\{1 - \frac{b_{u,i}(\tau)}{b_{l,i}(\tau)}\mathrm{e}^{-h\nu/[kT(\tau)]}\right\} B_{lu}\frac{n_{l,i}(\tau)}{n_i(\tau)} \times \int_0^\infty F_\nu(\tau)\varphi_{lu}(\nu, \tau)\,\mathrm{d}\nu. \tag{6}$$

Note that, the particle flux of the element associated with such definition of radiative acceleration would be[1]

$$J = \sum_i n_i v_i = \sum_i n_i D_i \frac{m}{kT}a_i, \tag{7}$$

where v_i and D_i are the ith ion diffusion velocity and diffusion coefficient, respectively.

The above expression for radiative acceleration includes the correction for stimulated emission, which is often omitted by other authors, as pointed out by Budaj (1994) and Seaton (1997), but does not include the redistribution effect pointed out by Montmerle & Michaud (1976) and generalized to include gravity by Alecian & Vauclair (1983). It has been substantially revisited by Gonzalez et al. (1995). The main idea of the redistribution effect is that, after the photon absorption, ion i is in excited state u and has a non-negligible probability $(1 - r_{u,i})$ of being ionized (mainly by collisions with fast electrons) before losing its momentum (mainly by collisions with protons). The probability of it remaining in state i is $r_{u,i}$ as the probability of recombination or further ionization is negligible. Momentum absorbed during the transition in the state i, p_{lu}, should then be redistributed to the two mass reservoirs mn_{i+1} and mn_i of $i+1$ and i ions in the proportions $(1 - r_{u,i})$ and $r_{u,i}$, respectively. Consequently, one finds[2]

$$a_i = \frac{1}{mn_i}\sum_{lu}\frac{\mathrm{d}p_{lu}}{\mathrm{d}t}r_{u,i} = \sum_{lu}a_{lu}r_{u,i} \tag{8}$$

$$a_{i+1} = \frac{1}{mn_{i+1}}\sum_{lu}\frac{\mathrm{d}p_{lu}}{\mathrm{d}t}(1 - r_{u,i}) = \sum_{lu}a_{lu}(1 - r_{u,i})\frac{n_i}{n_{i+1}}. \tag{9}$$

The redistribution function, $r_{u,i}$, depends on the ionization rate from the particular level, $\beta_{u,i}$, and the collision rate of the ion, β_i:

$$r_{u,i} = \frac{\beta_i}{\beta_{u,i} + \beta_i} = \frac{1}{\beta_{u,i}/\beta_i + 1}. \tag{10}$$

It is often useful to picture the radiative accelerations on many ions being applied via some effective radiative acceleration on the

[1] One can define the radiative acceleration in some other way as, for example, Seaton (1997), corresponding to different expressions for the particle flux.

[2] Note that these formulae are valid for our radiative accelerations, i.e. as defined by equation (4). Other formulae for the redistribution effect without a n_i/n_{i+1} factor would also hold but if combined with a slightly different definition of radiative acceleration, e.g. that of Seaton (1997).

element as a whole. Consequently, to compare the results with other authors and to display them, we also calculated the weighted mean radiative acceleration (although the results are stored for each ion and abundance separately). We adopted the following expression suggested by Gonzalez et al. (1995):

$$a(\tau) = \frac{\sum_i n_i D_i a_i}{\sum_i n_i D_i}, \tag{11}$$

where D_i is obtained from $D_{i,\mathrm{H\,I}}$, $D_{i,\mathrm{H\,II}}$, which are diffusion coefficients that describe the diffusion of the ith ion in neutral and ionized hydrogen, respectively:

$$\frac{1}{D_i} = \frac{1}{D_{i,\mathrm{H\,I}}} + \frac{1}{D_{i,\mathrm{H\,II}}}. \tag{12}$$

For the diffusion of the ith ion (excluding neutral) in protons we used (Aller & Chapman 1960):

$$D_{i,\mathrm{H\,II}} = \frac{1.947 \times 10^9 T^{5/2}}{n_{\mathrm{H\,II}} M_2 Z_i^2 A_1(2)}, \tag{13}$$

where $n_{\mathrm{H\,II}}$ is the proton number density, Z_i is the ionization degree (0 = neutral, etc.) and

$$A_1(2) = \ln\left(1 + x_{\mathrm{D}}^2\right); \quad M_2 = \frac{A}{1+A},$$

where A is the atomic weight in atomic mass units and

$$x_{\mathrm{D}} = \frac{4 d_{\mathrm{D}} kT}{Z_i e^2} \quad \text{and} \quad d_{\mathrm{D}} = \sqrt{\frac{kT}{4\pi n_{\mathrm{e}} e^2}},$$

where d_{D} is the Debye length and n_{e} is the electron number density. For the diffusion of neutrals in protons we used (Michaud, Martel & Ratel 1978)

$$D_{0,\mathrm{H\,II}} = 3.3 \times 10^4 \frac{T}{n_{\mathrm{H\,II}}} \sqrt{\frac{1+A}{\alpha A}}, \tag{14}$$

where α is the polarizability of neutral species ($\alpha = 0.395$, 0.667×10^{-24} cm^3 for Ne I and H I, respectively, from Teachout & Pack 1971). The same formula was used for the diffusion of ions in neutral hydrogen with $\alpha \rightarrow \alpha(\mathrm{H\,I})$ and $n_{\mathrm{H\,II}} \rightarrow n_{\mathrm{H\,I}}$, where $n_{\mathrm{H\,I}}$ is the neutral hydrogen number density. For the diffusion of neutrals in neutral hydrogen we used (Landstreet et al. 1998):

$$D_{0,\mathrm{H\,I}} = \frac{5.44 \times 10^3 \sqrt{T}}{n_{\mathrm{H\,I}}(\delta_{\mathrm{H\,I}} + \delta_i)^2} \sqrt{\frac{1+A}{A}}, \tag{15}$$

where $\delta_{\mathrm{H\,I}}$, δ_i are H I and diffusing atom diameters, respectively. The following values calculated using the method of Clementi, Raimondi & Reinhardt (1963)[3] were adopted: $\delta_{\mathrm{H\,I}} = 1.06 \times 10^{-8}$ cm, $\delta_{\mathrm{Ne\,I}} = 0.76 \times 10^{-8}$ cm.

2.2 Line selection and numerical calculations

As one goes from the envelope higher into the atmosphere, the electron density and associated Stark broadening drop sharply and the spectral lines become much narrower. One needs to consider fine structure to integrate the contributions from bound–bound transitions properly. Atomic data for the Ne I–IV lines were extracted from the Kurucz line list (Kurucz 1990, CDROM 23). However, one usually does not need to consider all the lines of the element and it is of high practical importance to select just the most important ones. Lines that are important for a particular atmosphere model were selected in the following way.

For practical purposes it is convenient to ascribe three characteristic Rosseland optical depths τ_1, τ_2, τ_3 or characteristic temperatures $T_1(\tau_1) \leqslant T_2(\tau_2) \leqslant T_3(\tau_3)$ to each ion i of the element of interest. The range T_1 to T_3 spans the region where the ion i is sufficiently populated and its contribution to the total radiative acceleration of the element is thus not negligible, while T_2 is the approximate temperature at which the ion dominates the element and the ith ion opacity is maximal. For each line lu of the ion i two parameters $RA_{i,lu,1}$ and $RA_{i,lu,3}$ were calculated, which correspond to two characteristic temperatures T_1, T_3:

$$RA_{i,lu,1,3} = 8.853 \times 10^{-13} m^{-1} \left[1 - \mathrm{e}^{-h\nu/(kT_{1,3})}\right] \times f_{lu} g_{l,i} \mathrm{e}^{-E_{l,i}/(kT_{1,3})} F_\nu(\tau_{1,3}), \tag{16}$$

where $E_{l,i}$ is the excitation potential of the lower level and

$$F_\nu(\tau_{1,3}) = \pi B_\nu(T_{\mathrm{eff}}) \quad \text{if} \quad T_{1,3} < T_{\mathrm{eff}}, \quad \text{or} \tag{17}$$

$$F_\nu(\tau_{1,3}) = \frac{4}{3} \frac{\pi}{\chi_{c,\nu}} \frac{\partial B_\nu(T)}{\partial T} \frac{\partial T}{\partial r} \text{ if } \quad T_{1,3} > T_{\mathrm{eff}}, \tag{18}$$

where B_ν is the Planck function, T_{eff} is the effective temperature and $\chi_{\mathrm{c},\nu}$ is the approximate continuous opacity after Borsenberger, Michaud & Praderie (1979).

The parameter $RA_{i,lu,1,3}$ is essentially a rough estimate of the expected radiative acceleration through weak lines, as equation (18) takes only opacity in the continuum into account and partition functions are set to 1.[4] Then we calculate a sum $RA_{i,1,3} = \sum_{lu} RA_{i,lu,1,3}$ through all the lines of the ith ion and skip the lines that do not contribute significantly to the sum. We ended up with about 10^3 Ne lines for a particular model atmosphere.

To evaluate numerically the integral in equation (6) it is necessary to estimate the integration step and integration boundaries. Thermal Doppler broadening at the coolest layer and classical radiative damping put constraints on the width of any spectral line and we use minimum frequency spacings equal to

$$\Delta\nu_{\mathrm{step}} \approx [\Delta\nu_{\mathrm{D}}(\tau_1) + \Gamma_{\mathrm{R}}/4\pi]/2, \tag{19}$$

where $\Delta\nu_{\mathrm{D}} = \nu c^{-1}\sqrt{2kT_1/m}$ and $\Gamma_{\mathrm{R}} = 2.47 \times 10^{-22}\nu^2$. Integration boundaries are associated with our linewidth, which is generally the broadest at the place of highest electron density owing to Stark broadening and we use

$$\Delta\nu_{\mathrm{w}} = k_1[\Gamma(\tau_3)/4\pi + \Delta\nu_{\mathrm{D}}(\tau_3)], \tag{20}$$

where

$$\Gamma(\tau_3) = \Gamma_{\mathrm{R}} + \Gamma_{\mathrm{S}}(\tau_3) + \Gamma_{\mathrm{W}}(\tau_3) \tag{21}$$

is the sum of the radiative, Stark and Van der Waals damping parameters. Here, k_1 is an adjustable constant for which numerical tests revealed that $k_1 \approx 2$–3 is high enough. This is, however, just the case of a weak line. If the opacity in the centre of our line is much greater than the opacity in the continuum one must usually integrate much further until the line opacity drops significantly below the continuum value. The reason why is apparent if one expresses the flux in equation (6) following the diffusion approximation and neglects continuum opacity; it is inversely proportional to the Voigt function.

[3] http://www.webelements.com/webelements.html

[4] The first simplification does not have any serious effect on this selection of the most important lines of a particular ion as it means we overestimate the expected accelerations through strong lines, so we cannot omit them. The second simplification also does not have any effect on line selection of an ion as $RA_{i,lu,1,3}$ or radiative accelerations for all the lines of a particular ion are scaled by the same value of ion population, which is proportional to its partition function. Again, it also means we cannot omit important lines.

Consequently, the integrand in equation (6) is a constant function of frequency. Only when the integration is carried far enough into the line wing, where continuum opacity again dominates, does the flux approach a constant function of frequency and the integrand sharply fall. Finally, the integration boundaries should be the maximum value of the mentioned effects:

$$\Delta\nu_{\rm width} = \pm\max[\Delta\nu_{\rm w}(\tau_3); \Delta\nu_{\rm s}(\tau_2)] \qquad (22)$$

where $\Delta\nu_{\rm s}(\tau_2)$ is defined for strong lines only and is $\Delta\nu$ for which the line opacity drops significantly below the continuum opacity at the depth where the involved ion population reaches its peak values. Typically, 40 to 10^3 frequency points were necessary to calculate the radiative acceleration through a Ne line.

The models adopted here were NLTE model atmospheres calculated with TLUSTY195 (Hubeny 1988; Hubeny & Lanz 1992, 1995) for standard solar composition and zero microturbulence. We treated H I, He I, He II, C I, C II, C III as explicit ions, which means that their level populations were solved in NLTE under the assumption of statistical equilibrium and their bound–bound, bound–free and free–free opacities were taken into account. Carbon was included as it is an important opacity source at cooler effective temperatures (Hubeny 1981). In Fig. 1 we plot the NLTE model against the Kurucz (1993) LTE line blanketed model for the same effective temperature and gravity. The two vertical bars point to the area where the continua around Ne I λ736 and Ne I λ6402 lines are formed. The first is a strong resonance line in the Lyman continuum and the second is in the Paschen continuum in the visible range. Abundance analyses of Ne have been performed using λ6402 (Dworetsky & Budaj 2000). The Lyman continuum is very opaque and models that go very high in the atmosphere are needed to solve for radiative transfer properly at these wavelengths.

$F_\nu(\tau)$ in equation (6) was calculated using the SYNSPEC36 and SYNSPEC42 (Hubeny, Lanz & Jeffery 1994) codes to solve the radiative transfer modified to obtain a non-standard output of flux at each frequency and depth (I. Hubeny, private communication), and to take into account the elements with atomic number >30 (Krtička 1998). This enabled us to take into account the bound–free and free–free opacity from explicit levels specified in the atmosphere model and the line blending using the full line list of Kurucz (1990). All the Kurucz lines with a line-to-continuum opacity ratio greater than 10^{-8} at $\tau = \max[1, \tau_2]$ were considered. All the resonance lines of Ne and other elements were calculated in approximate NLTE [allowing the source function to deviate from B_ν following the 'second-order escape probability method' of Rybicki (1984), see equation (25)].

Radiative accelerations were then calculated following equation (6) assuming $b_{u,i} = b_{l,i} = 1$ and LTE level populations. Partition functions were taken from the UCLSYN code (Smith & Dworetsky 1988; Smith 1992). Radiative accelerations were calculated for Ne I–IV and four abundances: 50 $A_\odot$, $A_\odot$, 10^{-2} $A_\odot$ and 10^{-5} $A_\odot$, where $A_\odot = 1.23 \times 10^{-4}$ and for the following model atmosphere parameters: $T_{\rm eff} = 11\,000$, 12 000, 13 000, 14 000, 15 000 K and $\log g = 4$, plus models with $T_{\rm eff} = 12\,000$ K and $\log g = 3.5$, 4.5. These are available in digital form in Budaj, Dworetsky & Smalley (2002) including a FORTRAN77 code containing the partition function routines.

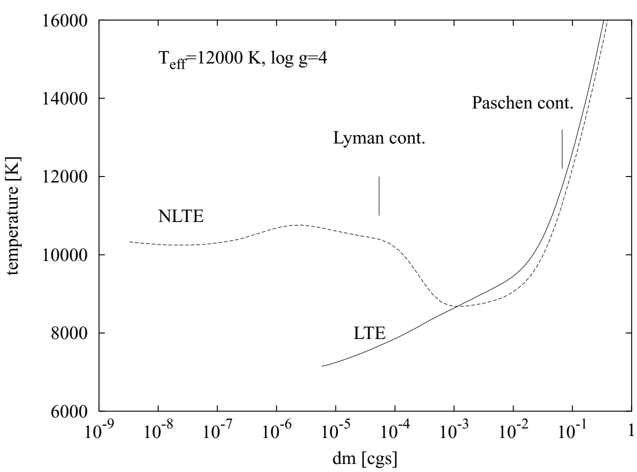

Figure 1. Temperature behaviour in a representative Kurucz's line-blanketed LTE and Hubeny's NLTE model atmosphere. Vertical bars indicate the unit monochromatic optical depth in the Lyman and Paschen continua close to the important Ne I λ736 and λ6402 transitions. As a depth coordinate we use 'dm' (g cm^{-2}), which is the mass of a column above a unit area at that depth in the atmosphere.

3 RESULTS AND DISCUSSION

3.1 Radiative accelerations on different Ne ions

The LTE populations of various Ne ions throughout the atmosphere are depicted in Fig. 2 for a representative atmosphere model with $T_{\rm eff} = 12\,000$ K, $\log g = 4$. Ne I is definitely dominant in the atmosphere. Ne IV becomes populated at the base of our models, while Ne II may dominate at very low densities and electron concentrations for d$m < 10^{-4}$ g cm^{-2}. However, above d$m < 10^{-3}$ g cm^{-2} strong departures of Ne ionization and excitation equilibrium from LTE occur (Sigut 1999) and our accelerations on different Ne ions should be considered as approximate above this level (see Fig. 9 in Section 3.6 for an illustration of expected deviations from the fully consistent NLTE case).

Accelerations in the representative model are plotted in Fig. 3. One can see that none of them exceeds the gravitational acceleration except at the very deepest layers. The acceleration on Ne I is strongest in the atmosphere where this ion is also most populated. The contribution of the neutral species such as Ne I to the total effective radiative acceleration of the element is both favoured by weighting with their diffusion coefficient (see equation 11), which is approximately two orders of magnitude larger than that

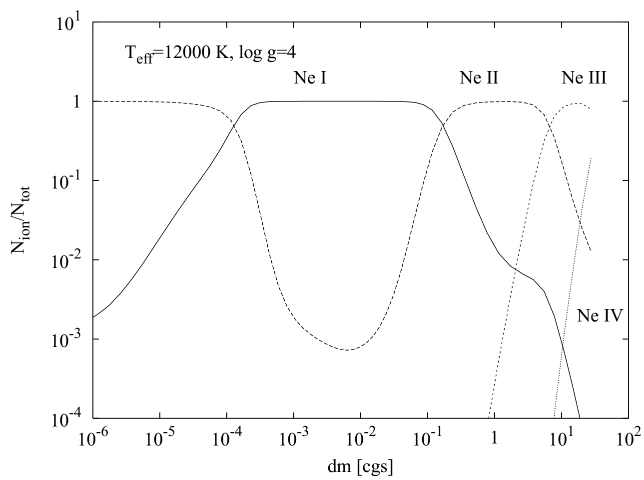

Figure 2. Ne ionization fractions in LTE in a representative NLTE model atmosphere.

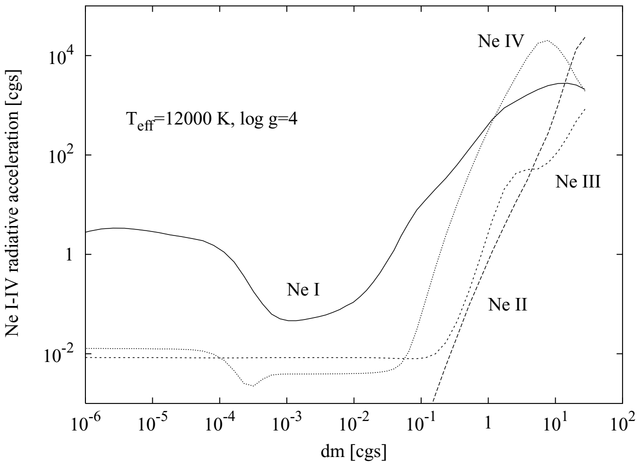

Figure 3. Radiative accelerations on Ne I–IV ions in a representative NLTE model atmosphere for the standard abundance of Ne. The downward gravitational acceleration of 10^4 cm s^{-2} is at least two to three orders of magnitude greater than the upward radiative acceleration throughout the photosphere.

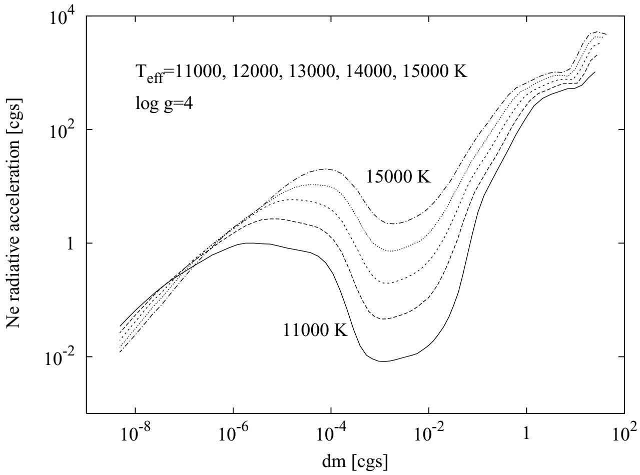

Figure 4. Radiative accelerations on Ne throughout the atmosphere as a function of stellar effective temperature and depth. Calculated for standard abundance of Ne.

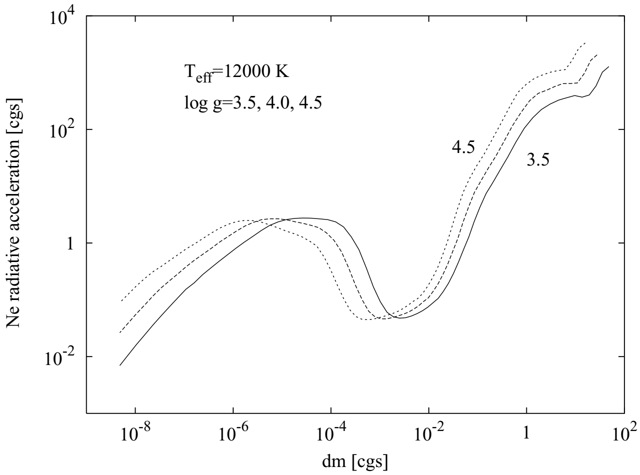

Figure 5. Radiative accelerations on Ne throughout the atmosphere as a function of stellar surface gravity and depth. Calculated for standard abundance of Ne.

for the charged species, and reduced by the redistribution effect. Nevertheless, acceleration of Ne I will be the most important contribution to the total acceleration not only in the atmosphere but also at rather great depth up to d$m \simeq 10$ g cm^{-2}. The low radiative accelerations found for Ne I are a consequence of its atomic structure because all resonance transitions, which are usually the most important ones, are in the Lyman continuum where Ne I atoms see little photon flux, while the rest of the lines originate from highly excited and weakly populated states. Nor can the redistribution effect discussed earlier increase the Ne I acceleration (see equation 8, and Fig. 7 in Section 3.4); just the opposite occurs. Radiative acceleration gained in the Ne I state is redistributed between Ne I and Ne II, which reduces the Ne I acceleration and adds it to the Ne II state where, however, the acceleration is not so effective owing to the much lower diffusion coefficient of ionized species; see equations (7) and (11).

We would like to stress that radiative acceleration (equation 6) on a particular ion is very sensitive to the partition functions. These are generally precise in the region where the ion dominates the element but have large uncertainties outside the region. Displaying effective accelerations overcomes the problem as partition functions drop out in equation (11) outside the region. Thus, if the reader wishes to use our radiative accelerations stored separately for each ion, the same partition functions should also be used.

3.2 Dependence on effective temperature and surface gravity

Now we can proceed further and explore how the situation changes with the effective temperature of the star. It is clear from Fig. 4 that the total acceleration rapidly increases with the effective temperature. However, within our range of interest it never exceeds the gravity in the line-forming region. Nevertheless, this suggests that Ne could accumulate at deeper layers in cooler stars than in hotter ones, the latter thus being more vulnerable to departures from the ideal stable atmosphere. Various mixing processes or radiatively driven stellar winds for which the intensity also increases with the effective temperature (Babel 1995; Krtička & Kubát 2001) might more easily enrich Ne in the atmospheres of much hotter stars. This resembles the case of He, which has an atomic structure similar to Ne. The abundance of He progressively increases with effective temperature from He-weak towards He-rich stars. This suggests that it might be interesting to search for Ne-rich analogues of He-rich stars among early B stars. On the other hand, for $T_{\rm eff} < 11\,000$ K, hydrogen becomes partially ionized, which triggers ambipolar diffusion and hydrogen superficial convective zones. This may also transport some Ne to the atmosphere from below. Our observations (Dworetsky & Budaj 2000) indicate that Ne underabundances are most pronounced in the middle of the HgMn domain and tend to be less extreme towards the cool and hot ends of the HgMn temperature region. This pattern could therefore be qualitatively expected. Observing Ne below $T_{\rm eff} = 11\,000$ K, however, becomes very difficult.

The radiative accelerations also depend on the surface gravity (Fig. 5). Lowering the surface gravity of the model shifts the radiative acceleration behaviour to deeper layers and reduces the radiative acceleration at the bottom of the atmosphere. However, the gravity-to-radiative acceleration ratio does not change very much and in this context effective temperature is a more important atmospheric parameter than $\log g$. Apparently, within the main sequence (approximately $3.5 \leqslant \log g \leqslant 4.5$), radiative acceleration of Ne never overcomes gravity.

3.3 Effects of homogeneous Ne abundance

Radiative acceleration on the element also depends on its abundance. This is a simple consequence of the fact that the energy flux in the integral in equation (6) depends on the element abundance. This is, however, only important in the case of strong lines where the line opacity is comparable to or larger than the opacity in the continuum. One can then expect that radiative acceleration will asymptotically increase as the element abundance decreases, until it reaches some maximum value corresponding to the sufficiently low abundance when all the element lines disappear and radiative acceleration will no longer be sensitive to the abundance (for more detail see Alecian & LeBlanc 2000). The situation is illustrated in Fig. 6. Surprisingly, the accelerations are very little dependent on abundance in the photospheres above d$m \simeq 0.1$ g cm^{-2} and do not exceed gravity for any abundance except at the extreme base of our models. Here a Ne deficit ranging from -0.5 dex for the hottest to -2 dex for the coolest model could be supported by radiation (i.e. radiative acceleration roughly equals gravity for this abundance and depth, d$m \approx 20$ g cm^{-2}). This weak abundance sensitivity results from the fact that resonance Ne I lines are not very strong because they are in the Lyman continuum where the continuous opacity is very large, effectively reducing the line-to-opacity ratio. We have found that contributions to the radiative acceleration of lines originating from excited Ne I levels are also important, but these weak lines do not introduce a strong dependence on the abundance because their line-to-continuum opacity ratio is low owing to the high excitation energies and low populations of the levels from which they originate. One can see from the figure that there is no abundance for which the radiative acceleration could balance the gravity in the line-forming region above d$m \simeq 0.1$ g cm^{-2}. The implication is that in this region, assuming a stable atmosphere devoid of any motion, Ne should sink and should be almost completely depleted and only its strong concentration gradient could balance the downward flux of Ne atoms. The Ne atom is at least an order of magnitude heavier than the mean 'molecular' mass of the gas, so the characteristic scale of the Ne abundance gradient would be an order of magnitude less than the pressure scaleheight, i.e. log d$m \approx 0.1$. Consequently, the fact that Ne is detected in most HgMn stars (Dworetsky & Budaj 2000) suggests the presence of some kind of instability competing with diffusion and suppressing the efficiency of diffusion processes.

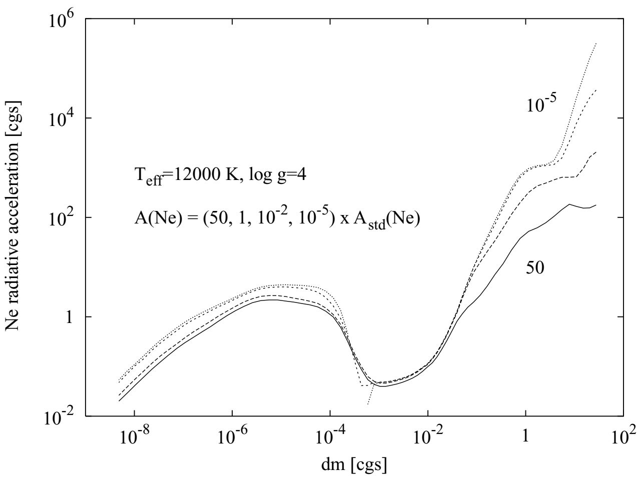

Figure 6. Radiative accelerations on Ne throughout the representative NLTE model atmosphere as a function of the homogeneous Ne abundance.

An example of such an instability is the weak stellar wind suggested by Landstreet et al. (1998).

One may also notice a sudden drop in the radiative accelerations at approximately $10^{-4} \leqslant$ d$m \leqslant 10^{-3}$ g cm^{-2}. This is not a numerical artefact but a very interesting effect when radiative acceleration may acquire negative values; this will be discussed in more detail below.

3.4 Redistribution effect

To take the redistribution effect into account properly one would need to calculate probabilities of all possible radiative and collisional transitions from the upper level to the continuum, including multiple cascade transitions as suggested by Gonzalez et al. (1995). That is a very difficult task and the above authors developed a method in which they set $r_{u,i} = 0$ for $n \geqslant 3$ and $r_{u,i} = 1$ for lower states. Thus their $r_{u,i}$ is a simple step function of level energy and does not depend on, for example, temperature. To cope with the problem and to estimate the influence of the redistribution effect we propose a slightly different and more general approach. The idea is simple. As mentioned in Section 2.1, collisions with electrons may change the ionization state before the momentum absorbed by the atom is lost in collisions with protons. Consequently, the redistribution function from a particular excited level depends mainly on the electron-to-proton collisional rates ratio. Higher atomic levels with energies corresponding to the electron kinetic energy $\approx kT$ below the ionization threshold are most strongly coupled to the continuum via collisional excitation and ionization. The probabilities of such processes are strongly temperature dependent via the Boltzmann factor $\mathrm{e}^{-\Delta E/kT}$ (Seaton 1962; Van Regemorter 1962) and still deeper atomic levels are affected as one goes deeper into the star. The electron-to-proton number density ratio almost does not change with depth in such hot stars and the Boltzmann factor thus embraces the essence of the electron to proton collisional rates ratio and one may write $\beta_{u,i}/\beta_i = C\mathrm{e}^{-\Delta E/BkT}$. Consequently, based on equation (10) we suggest the following expression for $r_{u,i}$:

$$r_{u,i} = \frac{1}{C\mathrm{e}^{-U} + 1} \quad \text{with} \quad U = (I_i - E_{u,i})\left(\frac{1}{A} + \frac{1}{BkT}\right) \qquad (23)$$

where I_i is the ith ion ionization potential and A, B, C are adjustable constants. It is beyond the scope of the present paper to calibrate precise values for the above-mentioned constants. B is most important as it parametrizes the temperature dependence and is of the order of 1. The $1/A$ term was introduced for those who prefer to use a Gonzalez et al. (1995) type of redistribution but do not like its step function shape and A is of the order of kT, but we use $A \rightarrow \infty$. C parametrizes the ratio of the total electron-to-proton collision rates. If $E_{u,i} \rightarrow I_i$ the level will register all electron impacts and $\beta_{u,i}/\beta_i = C$. Because electrons are $\sqrt{m_\mathrm{p}/m_\mathrm{e}}$ faster than protons, their collisions will be more frequent by approximately the same factor, and C is thus of the order of 40. The method of Gonzalez et al. (1995) is equivalent to the approximation of equation (23) by a step function and could be approached as a special case when $B \rightarrow \infty$ and $A \rightarrow 0$ or $A \rightarrow \infty$ depending on whether $E_{u,i} > I_i - E_\mathrm{crit}$ or $E_{u,i} < I_i - E_\mathrm{crit}$, respectively, where E_crit is some threshold energy. Note that $A \rightarrow 0$ means $r_{u,i} \rightarrow 1$, i.e. no redistribution at all and $A \rightarrow \infty$ means $r_{u,i} \rightarrow 1/(C+1) \rightarrow$ a small value, i.e. total redistribution is approached but never fully realized. Assuming that Gonzalez et al. (1995) took the lowest $n = 3$ level of C II as a cut-off in their calculation for $T = 31\,000$ K, which corresponds to $E_\mathrm{crit} = 80\,000$ cm^{-1} below continuum, we can simulate their method (using our equations 8 and 9 and forcing $r_{u,i} = 1$ or $r_{u,i} = 0$) and calibrate our method so that it would give $r_{u,i} = 0.5$ at

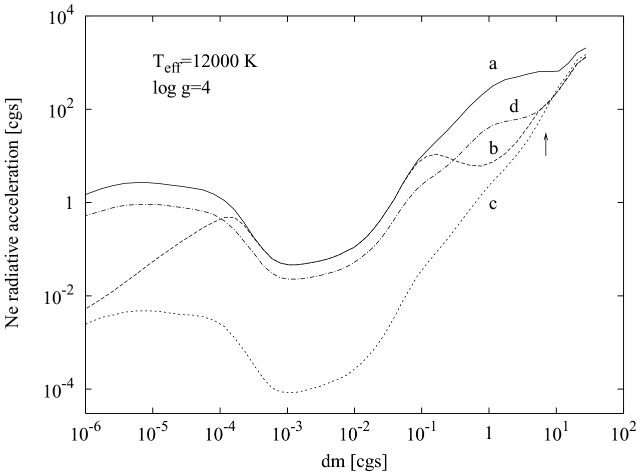

Figure 7. An illustration of the redistribution effect on the radiative accelerations on Ne throughout the representative NLTE model atmosphere as a function of depth calculated for standard homogeneous abundance of Ne. (a) no redistribution, solid line; (b) no redistribution and no diffusion coefficient weighting, dashes; (c) Gonzalez et al. (1995) type redistribution, dots; (d) our type redistribution, dash-dots. The arrow points to the depth where $T = 31\,000$ K.

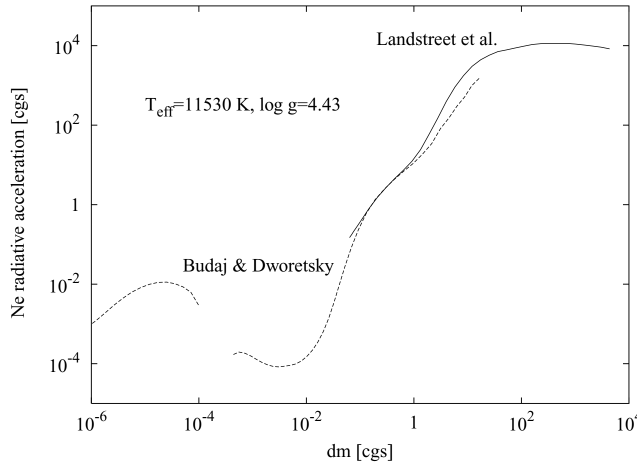

Figure 8. Comparison of our calculations in the atmosphere with those of Landstreet et al. (1998) in the envelope for the same model parameters. Here, for Ne I only resonance lines are considered. Both were calculated for standard abundances of Ne.

the same temperature. Assuming $C = 40$, $A \rightarrow \infty$ we obtain from equation (23) that $B = 1.0$ – a reasonable value indeed. Results of both methods are illustrated in Fig. 7 and one can see that while both methods may give similar results for $T = 31\,000$ K the Gonzalez et al. (1995) method strongly overestimates the redistribution effect for lower temperatures. A simple test of the redistribution effect treatment is recommended by calculating radiative accelerations without weighting them by diffusion coefficients (setting $D_i = 1$ for example in equation 11). This is because such accelerations are an invariant of the redistribution process.

3.5 Comparison with other work

We calculated an atmosphere model for $T_{\rm eff} = 11\,530$ K, $\log g = 4.43$, corresponding to one of the envelope models of Landstreet et al. (1998). Then we calculated the radiative accelerations, but in the case of Ne I we omitted all except the resonance lines, to simulate the assumption adopted by Landstreet et al. This assumption is not really justified as the omitted lines contribute significantly to the radiative acceleration. Inclusion of Ne I lines originating from excited levels, which absorb at the wavelengths where a star radiates much more than in the Lyman continuum, may increase the acceleration on Ne I by more than 1.5 dex. However, this does not have any serious consequences on the conclusions of Landstreet et al., as the radiative accelerations are so small they will still remain below that of gravity. The comparison is shown in Fig. 8. In this case we also considered $D_i = 1$ in equation (11) to follow their method. The agreement is quite good and small departures at the base of the atmosphere are mainly caused by slightly different temperature behaviour between our model atmosphere and their envelope model. The curious gap in our curve at $10^{-4} \leqslant {\rm d}m \leqslant 10^{-3}$ g cm^{-2} appears because the acceleration is negative here and cannot be plotted on a logarithmic scale.

3.6 NLTE effects

The aforementioned negative acceleration is a very interesting NLTE effect, which may lower still further the radiative accelerations on some ions in this part of the atmosphere. It is a consequence of the temperature inversion in the model atmosphere and the atomic structure of Ne I. As shown in Fig. 1, temperatures in the outer layers rise in a NLTE model for $10^{-4} \leqslant {\rm d}m \leqslant 10^{-3}$ g cm^{-2}. At this depth, and in these stars, the atmosphere is still optically thick in the Lyman continuum. Thus, according to the diffusion approximation, the star radiates into itself towards cooler regions at these wavelengths. If an element happens to have its important transitions in the Lyman continuum it may be pushed into the star by the radiation and its acceleration is thus negative. Similar effects can also be expected in the cores of very strong lines not necessarily in the Lyman continuum. To explore NLTE effects on the results we also calculated radiative accelerations on Ne I for three different assumptions in a representative NLTE model atmosphere with $T_{\rm eff} = 15\,000$ K, $\log g = 4$ and zero microturbulence.

(i) LTE case: neon populations in equation (6) are in LTE and the neon line source functions for flux calculations is equal to the Planck function

$$S_\nu = B_\nu. \tag{24}$$

(ii) Approximate NLTE: the same, but the line source function for resonance transitions is allowed to deviate from the Planck function following second-order escape probability methods

$$S_\nu = \sqrt{\frac{\epsilon}{\epsilon + (1-\epsilon)K_2(\tau)}}\,B_\nu, \tag{25}$$

where ϵ is the photon destruction probability and $K_2(\tau)$ is the kernel function (see Hubeny et al. 1994, the SYNSPEC manual, for more detail). Note that this option was used in the calculations described in Section 2.2 above.

(iii) Fully consistent NLTE case: with an NLTE model atmosphere, NLTE populations and NLTE source functions

$$S_\nu = \frac{2h\nu^3}{c^2}\left(\frac{g_{u,i}n_{l,i}}{g_{l,i}n_{u,i}} - 1\right)^{-1}. \tag{26}$$

In the full NLTE case the NLTE model atmosphere and Ne I level populations were calculated with TLUSTY195. As an input for TLUSTY195 we considered Hubeny's H I atom model with nine explicit levels and continuum, the 31-level Ne I atom model taken from

Table 1. Ne II energy levels considered. Column 1: level designation, column 2: ionization energy in cm^{-1}, column 3: statistical weight of the level. Energies are from Persson (1971).

Desig.	Energy	g
$2p^5\ ^2P^o$	330 445	6
$2p^6\ ^2S$	113 658	2
$3s\ ^4P$	111 266	12
$3s\ ^2P$	106 414	6

Dworetsky & Budaj (2000), and a simple four-level atom for Ne II with a continuum (Table 1). Generally, the data for Ne bound–bound and bound–free transitions were taken from the TOPbase (Cunto et al. 1993; Hibbert & Scott 1994), but Ne I oscillator strengths were from Seaton (1998). The MODION IDL interface written by Varosi et al. (1995) was particularly useful in constructing Ne I and Ne II atom models. Populations of those very high Ne I levels not included in our Ne I atom model were considered in LTE relative to the ground state of Ne II, the population of which was calculated in NLTE, when calculating the energy flux and acceleration. All Ne I level populations were set to LTE below d$m > 0.3$ g cm^{-2} when calculating the radiative accelerations.

The differences between the three assumptions are exhibited in Fig. 9 and become crucial for d$m < 10^{-3}$ g cm^{-2}, where the radiative accelerations in LTE and NLTE may differ by more than 3 dex. In the case of LTE we observe negative acceleration in the region of the temperature inversion. This was explained above. The approximate NLTE case is parallel to the LTE acceleration but about 1.5 dex smaller. This is caused by the difference in computed energy fluxes. While flux in the approximate NLTE case is real – lines are in absorption – and surprisingly close to the flux in the full NLTE case, the resonance Ne I lines are in emission in LTE as soon as the atmosphere becomes optically thin in the Lyman continuum and acceleration soars immediately. The difference between approximate NLTE and full NLTE originates mainly in the differences in level populations.

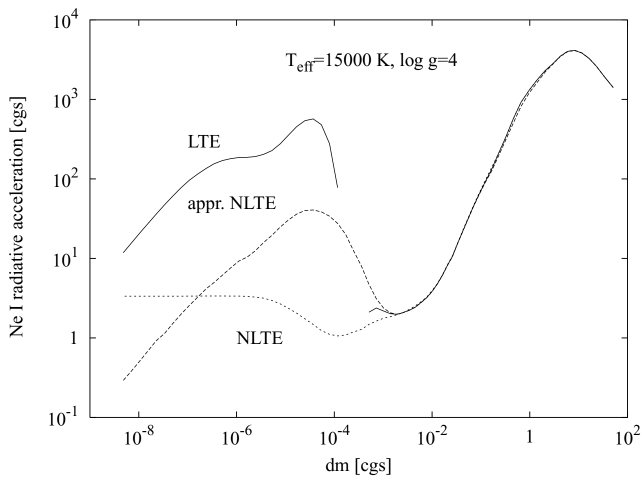

Figure 9. Comparison of radiative accelerations on Ne I obtained using different assumptions: LTE, approximate NLTE and full NLTE (see the text). Calculated for standard abundance of Ne.

4 SUMMARY

We have calculated radiative accelerations on Ne I–IV ions in the atmospheres of late B main-sequence stars. We take into account the fine structure and calculations include the effects of line blending using the whole Kurucz line list, bound–free and free–free opacity of explicit elements (H, He, C) as well as some NLTE effects. We explored how the acceleration changes with respect to effective temperature, surface gravity and homogeneous Ne abundance, and found that it is much smaller than gravity in and above the observed line-forming region. Only at the base of our models (d$m \simeq$ 20 g cm^{-2}) could a Ne deficit of about 0.5–2.0 dex be supported by the radiation, depending on the effective temperature. This implies that, in the stable atmospheres of late B stars, Ne should be almost completely depleted from the photosphere. This is qualitatively in agreement with the observations of Dworetsky & Budaj (2000), but the fact that we detected Ne in some HgMn stars suggests the presence of some weak transport or mixing mechanism contaminating the observed layers by Ne from the reservoir underneath. Possibly, this mechanism is associated with the partial hydrogen ionization at the cool end and a very weak stellar wind at the hot end of the HgMn T_{eff} span.

Finally, we demonstrated using a full NLTE calculation the importance of such effects on radiative accelerations and slightly improved a current treatment of the redistribution effect, which should be used in future calculations.

ACKNOWLEDGMENTS

We thank I. Hubeny and J. Krtička for patient discussions and help with the TLUSTY and SYNSPEC codes, B. Smalley for his work on fitting partition functions for UCLSYN, J. D. Landstreet and G. Alecian for discussing details concerning their calculations and an anonymous referee for many useful comments. JB gratefully acknowledges the support of the Royal Society/NATO fellowship scheme (Ref. 98B) and partial support by the VEGA grant no 7107 from the Slovak Academy of Sciences and APVT-51-000802 project.

REFERENCES

Adelman S.J., Pintado O.I., 2000, A&A, 354, 899
Adelman S.J., Snow T.P., Wood E.L., Evans I.I., Sneden C., Ehrenfreund P., Foing B.H., 2001, MNRAS, 328, 1144
Alecian G., LeBlanc F., 2000, MNRAS, 319, 677
Alecian G., Vauclair S., 1983, Fundamen. Cosmic Phys., 8, 369
Aller L.H., Chapman S., 1960, ApJ, 132, 461
Anders E., Grevesse N., 1989, Geochim. Cosmochim. Acta, 53, 197
Auer L.H., Mihalas D., 1973, ApJ, 184, 151
Babel J., 1995, A&A, 301, 823
Borsenberger J., Michaud G., Praderie F., 1979, A&A, 76, 287
Budaj J., 1994, in Zverko J., Žižňovský J., eds, CP and Magnetic Stars. Astronomical Institute, Slovak Academy of Sciences, Tatranská Lomnica, Slovakia, p. 72
Budaj J., Zboril M., Zverko J., Žižňovský J., Klačka J., 1993, in Dworetsky M.M., Castelli F., Faraggiana R., eds, ASP Conf. Ser. Vol. 44, Peculiar Versus Normal Phenomena in A-type and Related Stars. Astron. Soc. Pac, San Francisco, p. 502
Budaj J., Dworetsky M.M., Smalley B., 2002, Comm. Univ. London Obs. No 82, available at http://www.ulo.ucl.ac.uk/ulo_comms/82/index.html
Charbonneau P., Michaud G., 1988, ApJ, 327, 809
Clementi E., Raimondi D.L., Reinhardt W.P., 1963, J. Chem. Phys., 38, 2686
Cunto W.C., Mendoza C., Ochsenbein F., Zeippen C.J., 1993, A&A, 275, L5
Dworetsky M.M., Budaj J., 2000, MNRAS, 318, 1264

Gonzalez J.-F., LeBlanc F., Artru M.-C., Michaud G., 1995, A&A, 297, 223
Grevesse N., Noels A., Sauval A.J., 1996, in Holt S., Sonneborn G., eds, Cosmic Abundances. PASPC No. 99, p. 117
Hibbert A., Scott M.P., 1994, J. Phys. B, 27, 1315
Hubeny I., 1981, A&A, 98, 96
Hubeny I., 1988, Comput. Phys. Comm., 52, 103
Hubeny I., Lanz T., 1992, A&A, 262, 501
Hubeny I., Lanz T., 1995, ApJ, 439, 875
Hubeny I., Lanz T., Jeffery C.S., 1994, in Jeffery C.S., ed., Newsletter on Analysis of Astronomical Spectra No 20. CCP7; St Andrews Univ., p. 30
Hui-Bon-Hoa A., Alecian G., Artru M.-C., 1996, A&A, 313, 624
Hui-Bon-Hoa A., LeBlanc F., Hauschildt P.H., 2000, ApJ, 535, L43
Hui-Bon-Hoa A., LeBlanc F., Hauschildt P.H., Baron E., 2002, A&A, 381, 197
Krtička J., 1998, in Dušek J., Zejda M., eds, Proc. 20th Stellar Conf. Nicholas Copernicus Observatory and Planetarium, Brno, p. 73
Krtička J., Kubát J., 2001, A&A, 377, 175
Kurucz R.L., 1990, Trans. IAU, XXB, 168 (CD-ROM 23)
Kurucz R.L., 1993, ATLAS9 Stellar Atmosphere Programs and 2 km s^{-1} Grid (CD-ROM 13)
Landstreet J.D., Dolez N., Vauclair S., 1998, A&A, 333, 977
LeBlanc F., Michaud G., Richer J., 2000, ApJ, 538, 876
Michaud G., 1970, ApJ, 160, 641
Michaud G., 1982, ApJ, 258, 349
Michaud G., Martel A., Ratel A., 1978, ApJ, 226, 483
Montmerle T., Michaud G., 1976, ApJS, 31, 489
Persson W., 1971, Phys. Scr., 3, 133
Rybicki G.B., 1984, in Kalkofen W., ed., Methods of Radiative Transfer. Cambridge Univ. Press, Cambridge, p. 21
Sapar A., Aret A., 1995, A&A Trans., 7, 1
Seaton M.J., 1962, in Bates D., ed., Atomic and Molecular Processes. New York, Academic, p. 374
Seaton M.J., 1997, MNRAS, 289, 700
Seaton M.J., 1998, J. Phys. B, 31, 5315
Seaton M.J., 1999, MNRAS, 307, 1008
Sigut T.A.A., 1999, ApJ, 519, 303
Smith K.C., 1992, PhD thesis, Univ. London
Smith K.C., Dworetsky M.M., 1988, in Adelman S.J., Lanz T., eds, Elemental Abundance Analyses. Institut d'Astronomie de l'Univ. de Lausanne, Switzerland, p. 32
Teachout R.R., Pack R.T., 1971, At. Data, 3, 195
Van Regemorter H., 1962, ApJ, 136, 906
Varosi F., Lanz T., Dekoter A., Hubeny I., Heap S., 1995, MODION (NASA Goddard SFC), available at ftp://idlastro.gsfc.nasa.gov/pub/contrib/varosi/modion/

This paper has been typeset from a TEX/LATEX file prepared by the author.